IOPscience iopscience.iop.org

Home Search Collections Journals About Contact us My IOPscience

Magnetic field effects on current, electroluminescence and photocurrent in organic light-emitting diodes

This article has been downloaded from IOPscience. Please scroll down to see the full text article.

2007 J. Phys.: Condens. Matter 19 036209

(http://iopscience.iop.org/0953-8984/19/3/036209)

View the table of contents for this issue, or go to the journal homepage for more

Download details:
IP Address: 129.252.86.83
The article was downloaded on 28/05/2010 at 15:22

Please note that terms and conditions apply.

INSTITUTE OF PHYSICS PUBLISHING JOURNAL OF PHYSICS: CONDENSED MATTER

J. Phys.: Condens. Matter **19** (2007) 036209 (13pp) doi:10.1088/0953-8984/19/3/036209

Magnetic field effects on current, electroluminescence and photocurrent in organic light-emitting diodes

G Veeraraghavan[1], **T D Nguyen**[2], **Y Sheng**[2], **O Mermer**[2] **and M Wohlgenannt**[2,3]

[1] Department of Electrical and Computer Engineering and Optical Science and Technology Center, University of Iowa, Iowa City, IA 52242-1595, USA
[2] Department of Physics and Astronomy and Optical Science and Technology Center, University of Iowa, Iowa City, IA 52242-1595, USA

E-mail: gveerara@engineering.uiowa.edu, emailtho01@yahoo.com, yugang-sheng@uiowa.edu, omer-mermer@uiowa.edu and markus-wohlgenannt@uiowa.edu

Received 22 June 2006, in final form 21 November 2006
Published 5 January 2007
Online at stacks.iop.org/JPhysCM/19/036209

Abstract

We report on the experimental characterization of a recently discovered large magnetoresistive effect in polyfluorene and in Alq_3 organic light-emitting diodes. We also observe similar magnetic field effects (MFEs) of comparable magnitude in electroluminescence and photocurrent measurements. We provide a comprehensive overview of all these three types of MFE. To the best of our knowledge, the mechanism causing these MFEs is not currently known with certainty. Moreover, we show that experiments in bipolar, electroluminescent devices do not allow determination of whether the MFE acts on the carrier density or carrier mobility, making any attempt at explaining it ambiguous. As a remedy, we perform magnetoresistance measurements in hole-only polyfluorene devices and show that the MFE acts on the carrier mobility rather than carrier recombination.

1. Introduction

Organic π-conjugated semiconductors have been used to manufacture devices such as organic light-emitting diodes (OLEDs) [1, 2], photovoltaic cells [3–5] and field-effect transistors [6–8]. The inherent advantages in fabricating OLEDs by low temperature processing and solution processing make them very attractive for replacing the currently dominant display technology. There has been growing interest in spin [9–12] and magnetic field effects (MFEs) [13–23] in these materials. Frankevich and co-workers [24, 25] and Kalinowski and co-workers [26, 27] studied MFEs on electroluminescence (EL), photoconductivity (PC) and exciton dissociation at the electrodes in OLEDs. Davis *et al* [19] studied similar effects in organic devices with

[3] Author to whom any correspondence should be addressed.

 © 2007 IOP Publishing Ltd Printed in the UK

magnetic electrodes. All these works attributed the MFEs to excitonic processes. MFEs in a broader sense have also been extensively studied in radical chemistry. An excellent review can be found in [28].

We recently discovered [13] a large and intriguing magnetoresistive effect in polymer OLEDs, which we dubbed organic magnetoresistance (OMAR). We later showed that the effect also exists in OLEDs made from small molecules [14] and extended our characterization to a wide variety of polymers and small molecules [15]. OMAR has recently also been reported by another laboratory [29], and was interpreted using a model similar to that of Frankevich and Kalinowski. OMAR may find application in magnetic field sensors, e.g. in OLED pen-input interactive displays (patent pending, see demonstration video in [13]). In addition to its potential applications, OMAR poses a significant scientific puzzle since it is, to the best of our knowledge, the only known example of large room-temperature magnetoresistance in non-magnetic materials, with the exception of some high-mobility materials [30, 31].

In the present work we experimentally study MFE in polyfluorene (PFO), and tris-(8-hydroxyquinoline) (Alq_3) OLEDs using conductivity, electroluminescence and photoconductivity measurements. This will allow us to discuss the whole body of experimental MFE data on an equal footing and to extract conclusions from all three experiments and from the comparison between these three experiments. We also performed magnetoconductivity measurements on devices made with different exciton/carrier ratios and show that the observed MFE acts on carrier mobility rather than carrier recombination.

Electroluminescence in organic semiconductors results from the formation of excitons generated from free charge carriers. Usually, only spin-singlet excitons decay radiatively in OLEDs. Photoconductivity in organic semiconductors results from the transport of charges produced by intrinsic and/or extrinsic charge photogeneration [32, 33]. In intrinsic charge generation, the charges are produced by the dissociation of excitons generated by the photoexcitation in the bulk material without any aid from impurity levels. This requires that the large Coulomb attraction is somehow overcome, either involving hot carriers or thermal agitation.

2. Experimental details

The OMAR devices consist of a thin film of organic semiconductor sandwiched between a top and bottom electrode. The indium tin oxide (ITO, 40 nm) coated glass substrates were obtained from Delta Technologies. The substrates were cleaned in an ultrasonic bath using detergent solution, water and organic solvents followed by oxygen plasma cleaning and dried in nitrogen flow. The conducting polymer poly(3,4-ethylenedioxythiophene)-poly(styrenesulfonate) (PEDOT), purchased from H C Starck, was spin coated at 2000 revolutions per minute (rpm) on top of the ITO to provide an efficient hole injecting electrode. All other fabrication steps were carried out in a nitrogen glove-box. The active polymer PFO, obtained from American Dye Source, film was spin coated onto the PEDOT covered substrate to provide an organic semiconductor layer thickness of 150 nm from a chloroform solution. The active small molecule layer of Alq_3, obtained from H W Sands Corp., was thermally evaporated in high vacuum onto the PEDOT covered substrate, yielding an organic semiconductor layer thickness of $\approx$100 nm. A top contact of Ca (by thermal evaporation followed by a capping layer of Al by e-beam evaporation) was deposited at a base pressure of $\approx 1 \times 10^{-6}$ mbar on top of the organic semiconductor layer. The device area was ≈ 1 mm^2 for all the devices. The device structure used in our measurements was that of a typical single-layer OLED, i.e. metal/organic semiconductor/metal, as shown in figure 1 together with the schematic set-up for the various experiments.

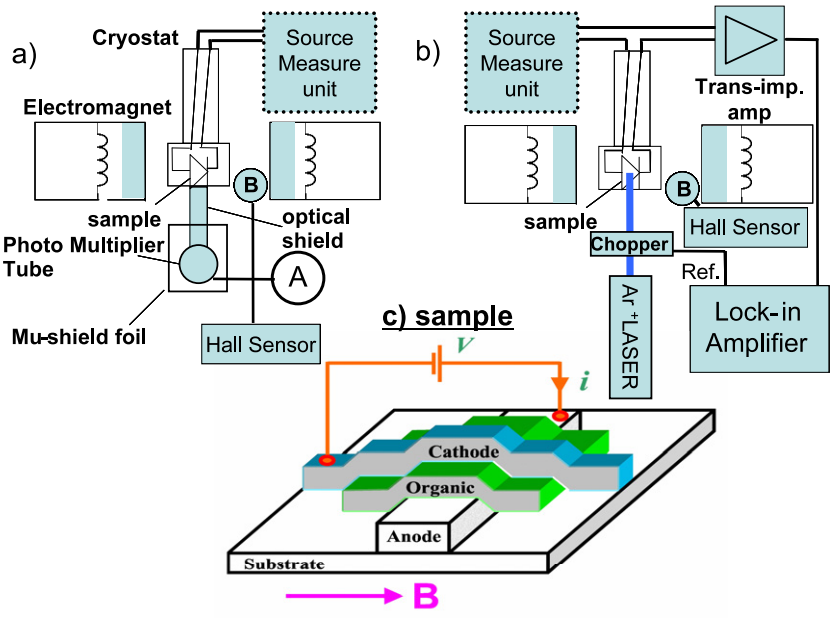

Figure 1. (a) Schematic drawing of the MFE on electroluminescence measurement. (b) Schematic drawing of the MFE on photocurrent measurement. (c) Schematic drawing of device sample and the magnetoresistance experiment.

(This figure is in colour only in the electronic version)

The samples were mounted on a closed cycle helium cryostat placed between the poles of an electromagnet. The magnetoconductance ratio was determined by measuring the change in current $\Delta I/I$ with magnetic field under constant bias voltage. The magnetoluminescence ratio was determined by measuring the change in EL with a photomultiplier tube that was shielded from the magnetic field using a high saturation mu-shield foil. The magnetic field effect on photocurrent was determined by measuring the change in photocurrent $\Delta PC/PC$ with magnetic field at constant bias voltages. The UV lines (364, 357 nm) from an argon ion laser were used to excite the device from the ITO side. A lock-in amplifier together with an optical chopper was used in measuring the photocurrent under forward and reverse bias. All measurements were done at room temperature and in dynamic vacuum provided by the cryostat. The data shown were measured with a magnetic field that was in plane with the device substrate, but we found that the effects are independent of the magnetic field direction.

3. Experimental results

Figure 2 shows the current–voltage characteristics (solid line) and the EL–voltage characteristics (scatter plot) of a PEDOT/PFO (≈150 nm)/Ca device. Figure 3 shows the same kind of data for a PEDOT/Alq_3 (≈100 nm)/Ca device. The insets show the molecular structure of the PFO and Alq_3. The current–voltage characteristic in OLEDs is non-linear and is usually interpreted using a model of space-charge-limited current in the presence of traps [34]. Figure 4 shows the current–voltage characteristics (solid line) and the photocurrent–voltage characteristics (scatter plot) of a similar PEDOT/PFO (≈150 nm)/Ca device. The inset shows the absorption spectrum of the device, with the arrow indicating the excitation photon energy

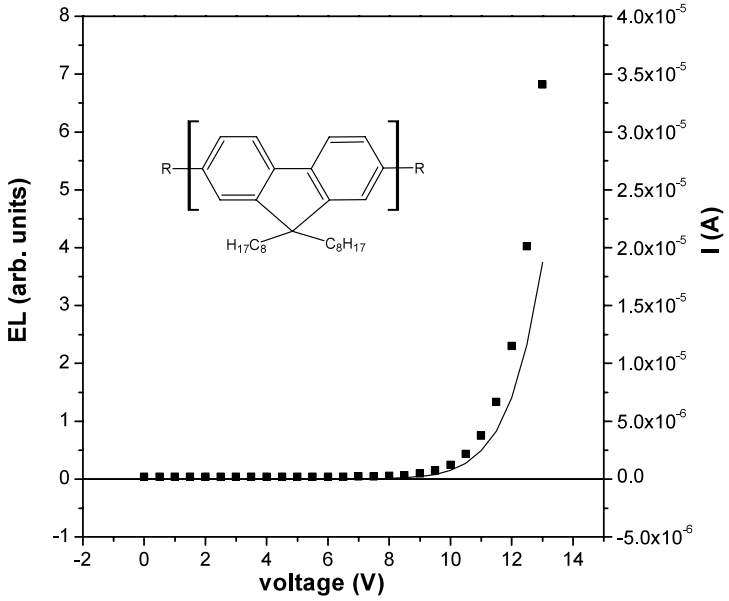

Figure 2. Current–voltage (solid line), EL–voltage (scatter plot) characteristics of ITO/PEDOT/PFO (≈150 nm)/Ca device at room temperature.

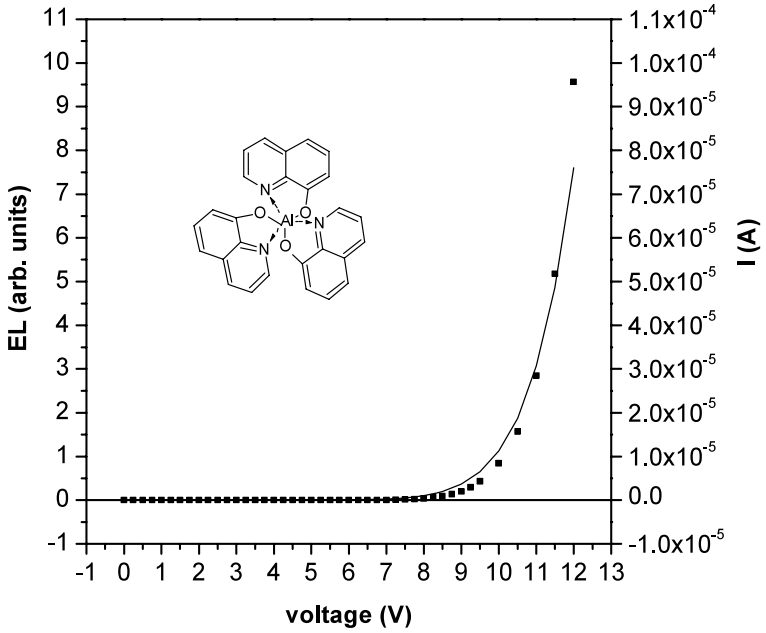

Figure 3. Current–voltage (solid line), EL–voltage (scatter plot) characteristics of ITO/PEDOT/Alq_3 (≈100 nm)/Ca device at room temperature.

used in photocurrent measurements. It follows from figure 4 that the PFO device absorbs most of the incident light at the excitation photon energy (3.4 eV) near the ITO electrode. A back-of-the-envelope calculation shows that the average photon is absorbed at a distance of 25% of

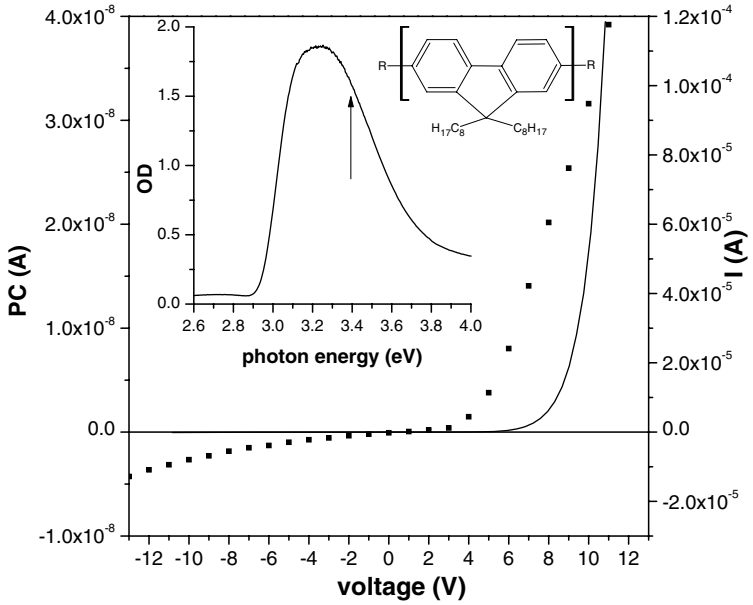

Figure 4. Current–voltage (solid line), photocurrent–voltage (scatter plot) characteristics of ITO/PEDOT/PFO (≈150 nm)/Ca device at room temperature. The inset shows the absorption spectrum of the device, with the arrow indicating the excitation wavelength (0.25 mW incident laser power) used in photocurrent measurements.

the device thickness from the ITO electrode. The figure shows that the photocurrent in the PFO device is much smaller when the ITO is under negative bias than when it is under positive bias.

Figure 5 shows the current–voltage characteristics (solid line) and the photocurrent–voltage characteristics (scatter plot) of a similar PEDOT/Alq_3 (≈100 nm)/Ca device. The figure 5 inset shows that the Alq_3 device absorbs the incident light weakly at the excitation photon energy (3.4 eV) and the light is therefore absorbed uniformly throughout the film. The uniform illumination leads to uniform bulk charge generation throughout the device, thereby preventing space-charge build-up. It is shown in figure 5 that the polarity of the bias does not affect the photocurrent magnitude as expected for bulk photogeneration in a uniformly illuminated device.

Figure 6 shows the measured MFEs on EL and current in a PFO sandwich device. The MFE on EL measured at constant current is also shown. The figure shows that we observed very large room-temperature magnetoconductance and magnetoluminescence in polymer PFO devices. It is seen that the magnetoluminescence ΔEL/EL and the magnetoconductance $\Delta I/I$ are of comparable magnitude and their shapes are equivalent. This suggests that both effects have a common origin. Figure 7 shows the MFEs on current (bold), current under illumination (dashed), $\Delta I/I$, photocurrent, ΔPC/PC, under forward bias (thin) at different bias voltages at room temperature. ΔPC/PC under reverse bias was not measured due to the very low photocurrent under reverse bias (figure 4). The magnitude of the ΔPC/PC is somewhat less than ΔEL/EL and $\Delta I/I$. Again, it should be noted that the ΔPC/PC and $\Delta I/I$ traces have the same width and shape, pointing to a common origin. The devices exhibited slow and gradual decay under laser illumination as observed by the increased biasing voltages required for similar currents and a gradually decreasing magnitude of OMAR. Therefore, $\Delta I/I$ in figure 7 is somewhat smaller than what we normally observe in PFO OLEDs. We note that the ΔPC/PC

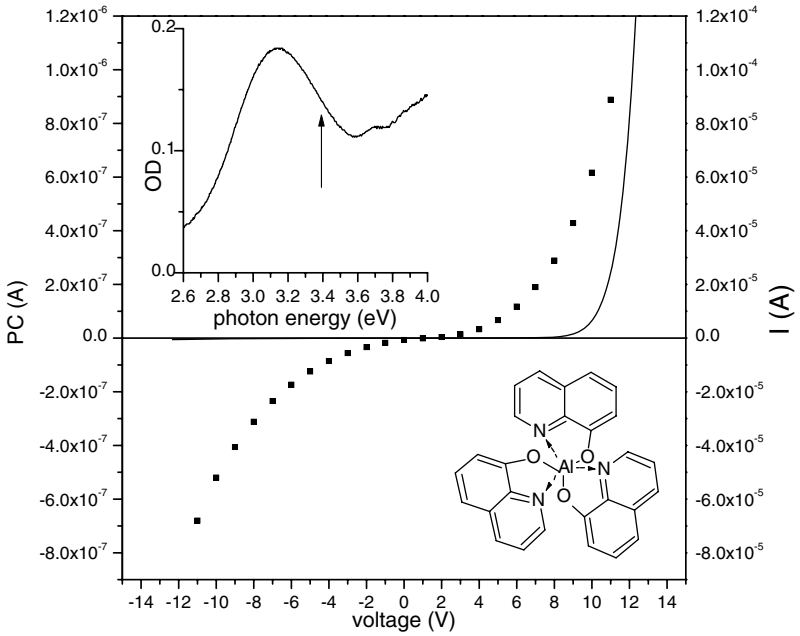

Figure 5. Current–voltage (solid line), photocurrent–voltage (scatter plot) characteristics of ITO/PEDOT/Alq_3 (≈100 nm)/Ca device at room temperature. The inset shows the absorption spectrum of the device with the arrow indicating the excitation wavelength (25 mW incident laser power) used in photocurrent measurements.

curves must be compared to the magnetoconductance traces under illumination (dotted lines) rather than the magnetoconductance curves in the dark (bold lines) for a comparison based on identical experimental conditions.

Figures 8 and 9 are the analogous figures for the Alq_3 sandwich device. In agreement with the results in PFO devices, the magnetoluminescence ΔEL/EL and the magnetoconductance $\Delta I/I$ are of comparable magnitudes and equivalent shapes, implying a common origin. Figure 9 shows the $\Delta I/I$, MFE on current (bold), current under illumination (dashed) and it also shows ΔPC/PC, under forward bias (thin) and reverse bias (dotted) at different bias voltages at room temperature. The magnitude of the ΔPC/PC is somewhat less than ΔEL/EL and $\Delta I/I$, in part due to slow but continuous degradation of the device under illumination.

4. Discussion

Because $\Delta I/I$, ΔPC/PC and ΔEL/EL show identical B dependences, they all are likely to share a common origin. Before examining the MFEs, let us review the basic formulae for the quantities we measured. I, PC and EL depend on carrier density and carrier mobility. The current density, J, is given by

$$J = e(p\mu_{\mathrm{p}} + n\mu_{\mathrm{n}})F \tag{1}$$

where e is the elementary charge, p and n are the densities of mobile positive and negative polarons, respectively, μ_p and μ_n are their respective mobilities and F is the electric field. These quantities may in general depend on the position, x.

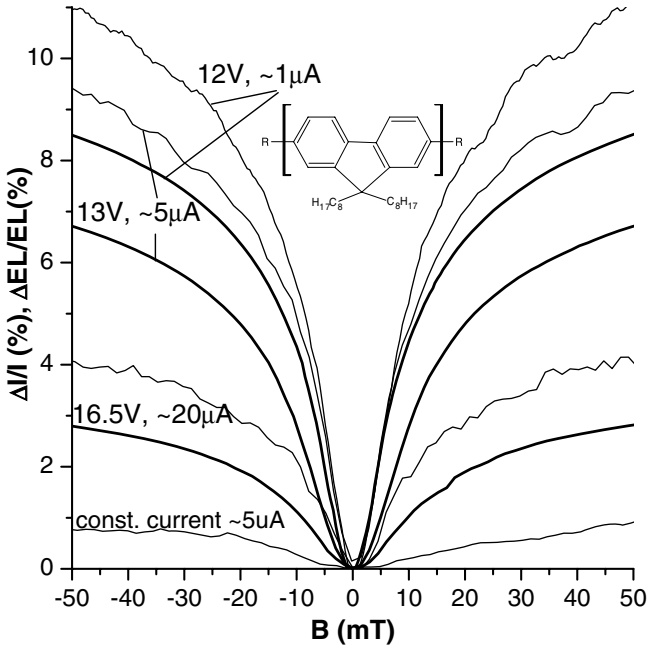

Figure 6. Magnetic field effect (MFE) on current (bold) and EL (thin) in a PEDOT/PFO (≈150 nm)/Ca device measured at several different constant voltages at room temperature. The MFE on EL measured at a constant current, 5 μA, corresponding to ≈13 V, is also shown.

The expression for EL is given by [17].

$$EL \propto \gamma pn \propto (\mu_{\mathrm{p}} + \mu_{\mathrm{n}})pn \tag{2}$$

γ is the electron–hole recombination constant, which is usually assumed to be given by the Langevin recombination formula [35],

$$\gamma = e(\mu_p + \mu_n)/\varepsilon\varepsilon_0, \tag{3}$$

where ε and ε_0 are the relative and absolute dielectric constants, respectively. The photocurrent density, J_{PC}, is given by

$$J_{\mathrm{PC}} = e(\delta p\mu_{\mathrm{p}} + \delta n\mu_{\mathrm{n}})F \tag{4}$$

where δ refers to a change in carrier density resulting from charge photogeneration, either intrinsic or extrinsic. It is therefore seen in equations (1), (2) and (4) that I, EL, and PC all depend on a combination of carrier density and mobility. Therefore, most generally, $\Delta I/I$, ΔEL/EL and ΔPC/PC can be caused either by an MFE on the carrier density or the mobility, thereby leading to a serious ambiguity in analysing the experiments and determining the mechanism causing OMAR. However, we note that the dependence of the EL on p and n is distinctly different from that of I and PC; it is proportional to their product rather than to their sum. Since MFEs of similar magnitude are observed in all three of the experiments, this suggests that the MFE acts on the mobilities rather than the carrier density. Nevertheless, we want to examine this issue more closely and will finally resolve it in the following. We note that since we have previously shown that OMAR is a bulk effect, rather than an effect on carrier injection [13], the only possibility for changing the carrier concentration is through their recombination. Indeed, Frankevich and others [24] and Kalinowski and co-workers [26, 27] have used an excitonic pair mechanism model based on hyperfine interaction in an attempt

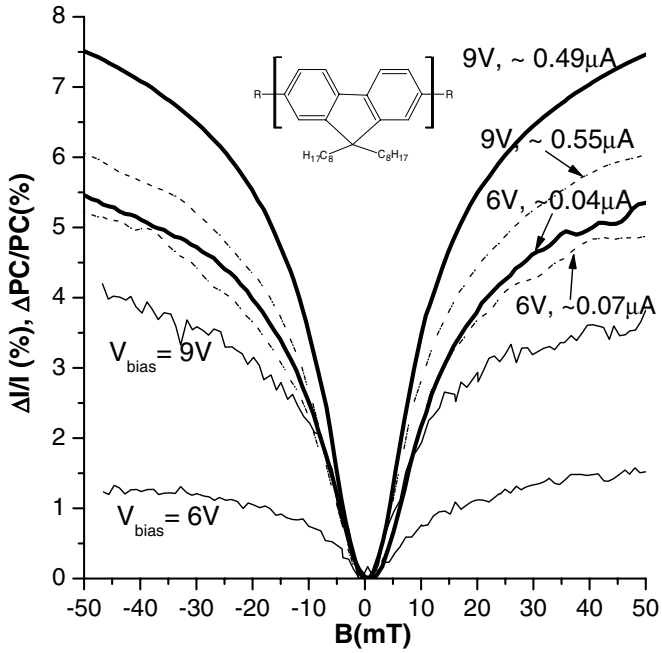

Figure 7. MFEs on current (bold), current under illumination (dashed) and photocurrent under forward bias (thin) in a PEDOT/PFO (≈150 nm)/Ca device measured at different bias voltages at room temperature.

to explain the origin of the MFEs on EL and photocurrent; i.e., they suggested an MFE mechanism that affects carrier recombination and thereby the carrier density. These models are in turn based on a more general framework developed in the field of radical chemistry, a review of which can be found in [28]. The Frankevich and Kalinowski models are based on spin-dependent recombination rates in singlet and triplet carrier pairs that are formed as an intermediate species during carrier recombination. The spin-dynamics induced by hyperfine coupling leads to enhanced recombination in *either* the singlet *or* triplet state. However, Reufer *et al* [36] have recently shown that the MFE on electroluminescence leads to *simultaneously enhanced* fluorescence (singlet) and phosphorescence (triplet) emission. This implies that the MFE affects both singlet and triplet channels equally, and it is in clear contradiction to the Frankevich/Kalinowski model, where one channel is enhanced at the expense of the other.

We have shown above that the experiments reported thus far are ambiguous. However, it is easy in principle to devise an experiment that does not suffer from this drawback: in a transport measurement in a unipolar OLED the carrier concentration is not subject to recombination, since no oppositely charged recombination partners (minority carriers) are available. One can control the injection of minority charge carriers by varying the corresponding electrode materials. The number of excitons formed in the device is proportional to the minority carrier concentration, whereas mostly the majority carriers determine the current density. This idea can be easily realized in hole-dominated PFO devices by choosing cathode (top electrode) materials with different work functions. PFO is widely known to be a hole transporter, and hence we control the minority carrier injection by fabricating PFO devices using Ca (excellent electron injector), Al and Au (very poor electron injector) as cathode materials. We note that whereas only data points for a single device of each type are shown the reported experiments

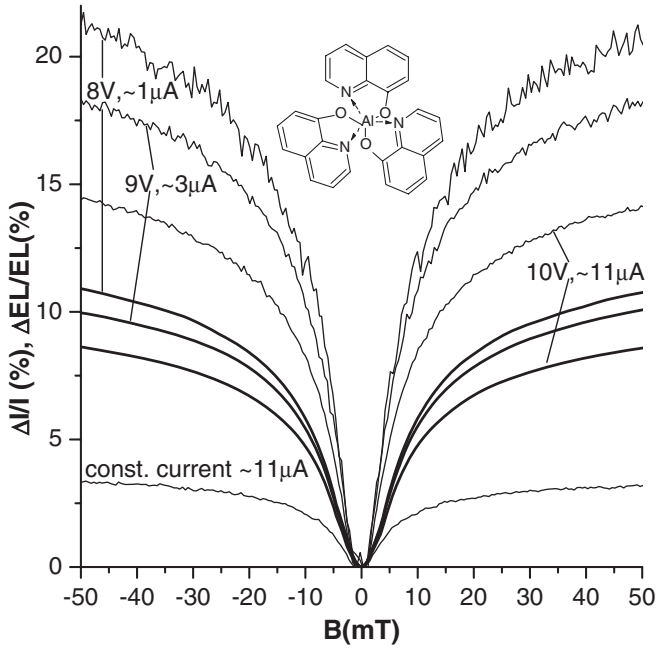

Figure 8. Magnetic field effect (MFE) on current (bold) and EL (thin) in a PEDOT/Alq_3 (≈100 nm)/Ca device measured at several different constant voltages at room temperature. The MFE on EL measured at a constant current, 11 μA, corresponding to ≈10 V, is also shown.

were repeated several times and very reproducible results were obtained. Figure 10 shows the current–voltage characteristics (figure 10(c)), the measured EL intensity as a function of I (figure 10(b)) and the magnitude of $\Delta I/I$ as a function of the exciton/carrier ratio η_1 (figure 10(a)). The exciton/carrier ratio, η_1, was inferred from the data shown in panel (b), where we found that the magnitude of EL, at a given current, in Ca devices is about one order of magnitude larger than that in Al devices, and about three orders of magnitude larger than in Au devices. This is well known [1] to result from the mismatch of the cathode work function and the polymer's conduction band in the case of Al and Au cathodes. Correspondingly, η_1 is one (three) orders of magnitude lower in Al (Au) devices compared to Ca devices.

At first glance figure 10(a) seems to imply an excitonic origin of OMAR since the magnitude of $\Delta I/I$ increases as the exciton/carrier ratio, η_1, increases. However, on closer inspection it is seen that the increase is much weaker than the linear dependence one would expect if OMAR were indeed caused by an excitonic phenomenon. We find $\Delta I/I \alpha \eta_1^{\alpha}$, where α ranges from $1/3$ to $1/2$. If OMAR were not related to an excitonic effect there should be no dependence on η_1 at all. However, the observed weak dependence is not unexpected. It is possible that the interface resistance of polymer/Au is larger than that of polymer/Ca, resulting in additional resistance. Au is indeed known [37] for producing non-Ohmic contacts with polymers either due to inferior wetting or the high temperature evaporation damaging the polymer layer. This interface resistance is not subject to OMAR and hence the magnitude of OMAR decreases. Figure 10(c) indeed shows that changing the cathode affects not only the η_1 but also changes the device resistance greatly. Moreover, in unipolar devices space-charge limited current conditions occur, which are possibly unfavourable for OMAR. In bipolar devices, however, the space charges of the two carrier types partially cancel each other. In summary, if OMAR were due to MFEs on charge recombination (EL) there should be a linear

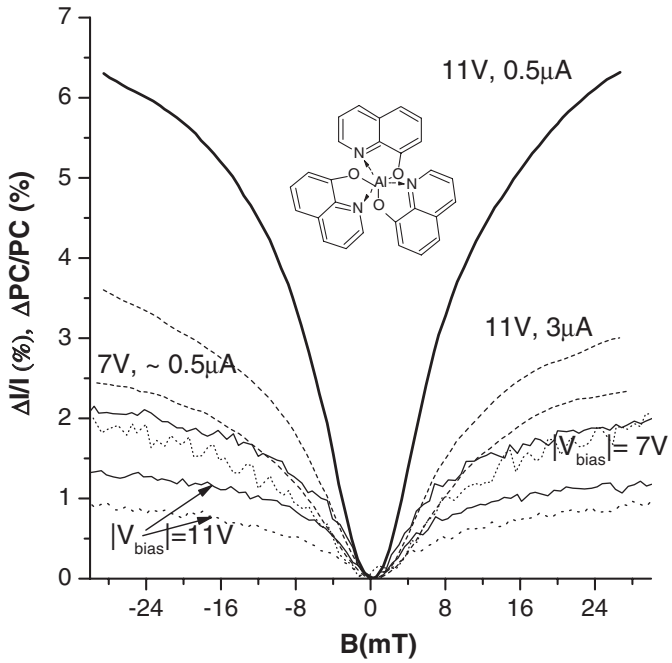

Figure 9. MFEs on current (bold), current under illumination (dashed) and photo current under forward bias (thin) and reverse bias (dotted) in a PEDOT/Alq_3 (≈100 nm)/Ca device measured at different bias voltages at room temperature.

dependence between OMAR and exciton density. Our measurements therefore show that OMAR is most likely not related to MFEs on charge recombination but is due to MFEs on mobility.

We believe that this conclusion is highly important, since it excludes any of the well known MFE mechanisms as a potential explanation of OMAR. To the best of our knowledge, these mechanisms [28] all rely on the formation of pairs and break down if pairs do not form. Whereas the formation of pairs is plausible in the case of oppositely charged partners that will be attracted to each other by the Coulomb force, it is counterintuitive in the case of repulsive interaction in unipolar devices. Moreover, a standard textbook treatment shows that in the commonly employed Langevin formalism of recombination the rate-limiting step occurs at the moment when carriers diffuse from outside the Coulomb radius, $r_C = e^2/4\pi\varepsilon\varepsilon_0 kT$, where the binding energy equals the thermal energy, to within this border. The carriers cross this border in an uncorrelated manner at a rate equal to $4\pi Dr_C n$, where D is the diffusion constant. Because r_C, which equals ≈20 nm at room temperature, is much larger than the range of the exchange interaction, the spins of the recombining carriers are not correlated during the rate-limiting recombination step. Furthermore, Langevin recombination gives a bimolecular rate, whereas pair recombination is, mathematically speaking, a monomolecular event. This is because the recombination rate for a particular carrier, once paired, is independent of the density of potential recombination partners since it has already selected its recombination partner and excluded all others. Pair mechanism models should therefore not be applicable to recombination of non-geminate carriers in OLEDs, which are believed to recombine through Langevin recombination [38]. Pair mechanism models can, however, be relevant to treating geminate recombination, as it occurs e.g. in PC experiments. However, our experimental

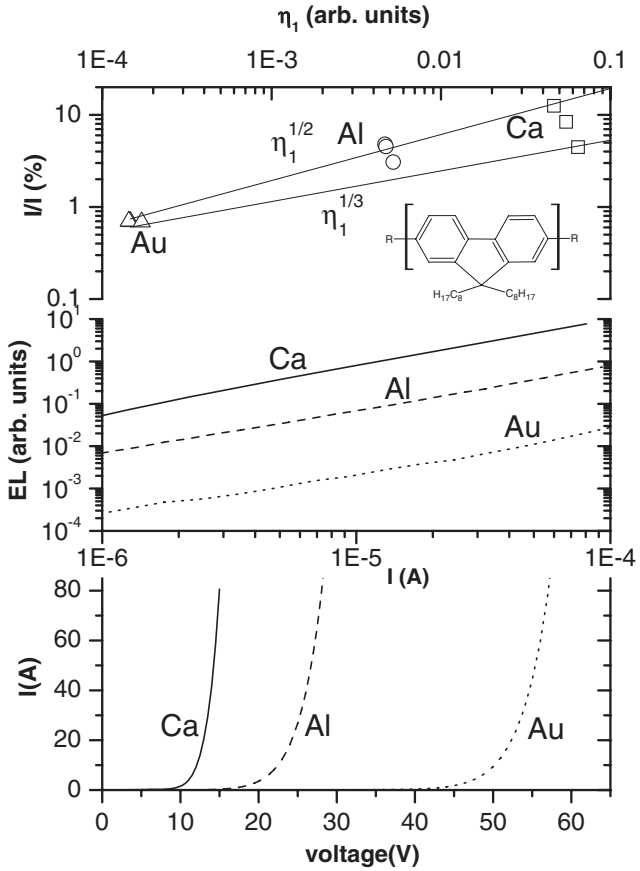

Figure 10. (a) $\Delta I/I$ at $B = 100$ mT in several PEDOT/PFO (≈150 nm)/cathode devices with Ca, Al or Au as the cathode as a function of the exciton/carrier ratio η_1. (b) EL as a function of current. (c) Current–voltage (I–V) characteristics. All data were obtained at room temperature.

observation that the MFE is of similar magnitude in both PC and conductivity measurements suggests that pair mechanism models are not important in PC measurements in OLEDs either, at least in the materials studied here.

We therefore believe that OMAR is a phenomenon, although superficially similar to pair mechanism MFE, which requires a different explanation. This is demonstrated most dramatically in our measurements in unipolar devices, where the attractive interaction necessary to form pairs does not exist. Moreover, we have previously shown [39] that even in a bipolar device pair mechanism models based on an attractive interaction contradict several important experimental facts. In our recent, unfinished work we have identified a potential mechanism which we believe to be in agreement with experimental observations. Its details will be reported elsewhere. Briefly, it is based on carrier hopping and assumes that the hopping sites can be either unoccupied, singly occupied or doubly occupied, and that double occupation is only allowed in a singlet configuration. Sites close to the Fermi energy may already be occupied, and hopping onto these sites can therefore occur only in an overall singlet state. The density of potential target sites for hops is therefore restricted by Pauli's principle, and this restriction is partially lifted in the case of mixing of Zeeman states by the hyperfine interaction. We have outlined this mechanism in a recent cond-mat archive paper [40].

5. Conclusion

We have provided a comprehensive overview of the magnetic field dependence of current, photocurrent and EL in OLEDs made from Alq_3 and PFO. Magnetic field effects of comparable magnitude (up to 10% at 10 mT at 300 K) were observed in all three experiments. We showed that there exists a serious ambiguity regarding the interpretation of these effects, since both mobility and carrier density enter the phenomenological equations for current, photocurrent and electroluminescence. We therefore performed magnetoconductivity measurements on devices made with different exciton/carrier ratios and showed that the observed effects are due to a magnetic field effect on mobility rather than charge recombination. However, the exact mechanism that results in the observed magnetic field dependence of the mobility still needs to be worked out.

Acknowledgments

We acknowledge fruitful and inspiring discussions with Professors P A Bobbert and M E Flatté. This work was supported by NSF grant No ECS 04-23911.

References

[1] Friend R H *et al* 1999 *Nature* **397** 121
[2] Forrest S R 2004 *Nature* **428** 911–8
[3] Brabec C J, Sariciftci N S and Hummelen J C 2001 *Adv. Funct. Mater.* **11** 15–26
[4] Peter Peumans S R F, Uchida S and Forrest S R 2003 *Nature* **425** 158–62
[5] Granstrom M, Petritsch K, Arias A C, Lux A, Anderson M R and Friend R H 1998 *Nature* **395** 257–60
[6] Dimitrakopoulos C D and Malenfant P R L 2002 *Adv. Mater.* **14** 99–117
[7] Gundlach D J, Lin Y Y and Jackson T N 1997 *IEEE Electron. Device Lett.* **18** 87–9
[8] Shtein M, Mapel J, Benziger J B and Forrest S R 2002 *Appl. Phys. Lett.* **81** 268–70
[9] Wohlgenannt M, Tandon K, Mazumdar S, Ramasesha S and Vardeny Z V 2001 *Nature* **409** 494–7
[10] Dediu V, Murgia M, Matacotta F C, Taliani C and Barbanera S 2002 *Solid State Commun.* **122** 181–4
[11] Xiong Z H, Wu D, Vardeny Z V and Shi J 2004 *Nature* **427** 821
[12] Hu B, Wu Y, Zhang Z, Dai S and Shen J 2006 *Appl. Phys. Lett.* **88** 022114
[13] Francis T L, Mermer O, Veeraraghavan G and Wohlgenannt M 2004 *New J. Phys.* **6** 185
[14] Mermer O, Veeraraghavan G, Francis T L and Wohlgenannt M 2005 *Solid State Commun.* **134** 631–6
[15] Mermer O, Veeraraghavan G, Francis T L, Sheng Y, Nguyen D T, Wohlgenannt M, Kohler A, Al-Suti M and Khan M 2005 *Phys. Rev.* B **72** 205202
[16] Mermer O, Veeraraghavan G, Francis T L and Wohlgenannt M 2003 *Preprint* cond-mat/0312204
[17] Kalinowski J 1999 *J. Phys. D: Appl. Phys.* **32** R179–249
[18] Kalinowski J, Cocchi M, Virgili D, Fattori V and Marco P D 2004 *Phys. Rev.* B **70** 205303
[19] Davis A H and Bussmann K 2004 *J. Vac. Sci. Technol.* A **22** 1885–91
[20] Yoshida Y, Fujii A, Ozaki M, Yoshino K and Frankevich E L 2005 *Mol. Cryst. Liquid Cryst.* **426** 19–24
[21] Salis G, Alvarado S F, Tschudy M, Brunschwiler T and Allenspach R 2004 *Phys. Rev.* B **70** 085203
[22] Prigodin V N, Raju N P, Pokhodnya K I, Miller J S and Epstein A J 2002 *Adv. Mater.* **14** 1230–3
[23] Raju N P, Savrin T, Prigodin V N, Pokhodnya K I, Miller J S and Epstein A J 2003 *J. Appl. Phys.* **93** 6799–801
[24] Frankevich E, Lymarev A, Sokolik I, Karasz F, Blumstengel S, Baughman R and Hoerhold H 1992 *Phys. Rev.* B **46** 9320–4
[25] Frankevich E, Zakhidov A, Yoshino K, Maruyama Y and Yakushi K 1996 *Phys. Rev.* B **53** 4498–508
[26] Kalinowski J, Szmytkowski J and Stampor W 2003 *Chem. Phys. Lett.* **378** 380–7
[27] Kalinowski J, Cocchi M, Virgili D, Di Marco P and Fattori V 2003 *Chem. Phys. Lett.* **380** 710–5
[28] Steiner U E and Ulrich T 1989 *Chem. Rev.* **89** 51
[29] Prigodin V N, Bergeson J D and Lincoln D M 2006 *Synth. Met.* **156** 757–61
[30] Xu R, Husmann A, Rosenbaum T F, Saboungi M L, Enderby J E and Littlewood P B 1997 *Nature* **390** 57–60
[31] Chien C L, Yang Y, Liu K, Reich D H and Searson P C 2000 *J. Appl. Phys.* **87** 9
[32] Daubler T K, Neher D, Rost H and Horhold H H 1999 *Phy. Rev.* B **59** 1964–72

[33] Goodman A M and Rose A 1971 *J. Appl. Phys.* **42** 2823–30
[34] Blom P W M *et al* 2000 *Mater. Sci. Eng.* R **27** 53–94
[35] Pope M and Swenberg C E 1999 *Electronic Processes in Organic Crystals* (New York: Clarendon)
[36] Reufer M, Walter M J, Lagoudakis P G, Hummel A B, Kolb J S, Roskos H G, Scherf U and Lupton J M 2005 *Nat. Mater.* **4** 340–6
[37] Campbell A J, Bradley D and Antoniadis H 2001 *Appl. Phys.* **89** 3343–51
[38] Blom P W M, DeJong M J M and Breedijk S 1997 *Appl. Phys. Lett.* **71** 930–2
[39] Sheng Y, Nguyen T D, Veeraraghavan G, Mermer O, Wohlgenannt M, Qui S and Scherf U 2006 *Phy. Rev.* B **74** 045213
[40] Wohlgenannt M and Bobbert P A 2006 *Preprint* cond-mat/0609592